OXFORD

ORIGINAL ARTICLE

Lesions to the Fronto-Parietal Network Impact Alpha-Band Phase Synchrony and Cognitive Control

Sepideh Sadaghiani [1,2,3], Pascasie L. Dombert[3,4], Marianne Løvstad[5,6], Ingrid Funderud[5], Torstein R. Meling[7], Tor Endestad[5,8], Robert T. Knight[3], Anne-Kristin Solbakk[5,7,8] and Mark D'Esposito[3]

[1]Psychology Department, University of Illinois at Urbana-Champaign, 61801 Urbana, IL, USA, [2]Beckman Institute for Advanced Science and Technology, University of Illinois at 61801 Urbana-Champaign, Urbana, IL, USA, [3]Department of Psychology, Helen Wills Neuroscience Institute, University of California, 94720 Berkeley, CA, USA, [4]Psychology and Neuroscience Programme, Maastricht Universirty, 6229 ER Maastricht, The Netherlands, [5]Department of Psychology, University of Oslo, 0373 Oslo, Norway, [6]Department of Research, Sunnaas Rehabilitation Hospital, 1453 Nesodden, Norway, [7]Department of Neurosurgery, Oslo University Hospital, Rikshospitalet, 0373 Oslo, Norway and [8]Department of Neuropsychology, Helgeland Hospital, 8657 Mosjøen, Norway

Address correspondence to Sepideh Sadaghiani. Email: sepideh.sadaghiani@gmail.com ⓘ orcid.org/0000-0001-8800-3959

Abstract

Long-range phase synchrony in the α-oscillation band (near 10 Hz) has been proposed to facilitate information integration across anatomically segregated regions. Which areas may top-down regulate such cross-regional integration is largely unknown. We previously found that the moment-to-moment strength of high-α band (10–12 Hz) phase synchrony co-varies with activity in a fronto-parietal (FP) network. This network is critical for adaptive cognitive control functions such as cognitive flexibility required during set-shifting. Using electroencephalography (EEG) in 23 patients with focal frontal lobe lesions (resected tumors), we tested the hypothesis that the FP network is necessary for modulation of high-α band phase synchrony. Global phase-synchrony was measured using an adaptation of the phase-locking value (PLV) in a sliding window procedure, which allowed for measurement of changes in EEG-based resting-state functional connectivity across time. As hypothesized, the temporal modulation (range and standard deviation) of high-α phase synchrony was reduced as a function of FP network lesion extent, mostly due to dorsolateral prefrontal cortex (dlPFC) lesions. Furthermore, patients with dlPFC lesions exhibited reduced cognitive flexibility as measured by the Trail-Making Test (set-shifting). Our findings provide evidence that the FP network is necessary for modulatory control of high-α band long-range phase synchrony, and linked to cognitive flexibility.

Key words: cognitive flexibility, dorsolateral prefrontal cortex, fronto-parietal network, lesion, alpha oscillations

Introduction

Functional connectivity across anatomically segregated brain regions is central to information processing at all levels from perception and action to higher cognitive functions (Varela et al. 2001; Singer 2013). For this information exchange, cross-regional neuronal ensembles must form and re-shape adaptively on a fast time scale. Synchronization of oscillatory activity across neuronal populations is a particularly well-suited

mechanism for such information integration (Varela et al. 2001; Uhlhaas et al. 2009; Wang 2010). α-band oscillations (~8–12 Hz) play an important and prominent role in this context because their oscillation phase has a uniquely strong influence on cortical excitability, with a maximal inhibitory impact at the peak of the α-phase cycle (Klimesch et al., 2007; Mazaheri and Jensen 2010; Haegens et al. 2011; Mathewson et al. 2011). Synchronization of these excitability cycles across regions can thus temporally align segregated blocks of information to facilitate their integration (Palva and Palva 2011). Indeed, increased cross-regional α-band phase synchronization has been reported to support numerous cognitive processes including low- and high-level perception, mental imagery, working memory, and cognitive set-shifting, especially when top-down control demands are increased (von Stein and Sarnthein 2000; Mima et al. 2001; Sauseng et al. 2005; Doesburg et al. 2009; Palva et al. 2010; Zanto et al. 2011; Pang et al. 2016; Lobier et al. 2018). As a mechanism for cross-regional integration, α-band phase synchronization is likely under control of higher-order brain regions that modulate communication between primary processing areas according to current demands. What specific higher-order control regions may exert such top-down modulation of α-band phase synchronization is largely unknown.

In a previous study, we identified a large-scale fronto-parietal (FP) control network as a likely candidate for regulating long-range α-band phase synchronization (Sadaghiani et al. 2012). Using simultaneously recorded electroencephalography (EEG) and functional magnetic resonance imaging (fMRI) during resting wakefulness, we determined which brain regions' activity (measured by fMRI) correlated with spontaneous fluctuations in oscillatory phase synchrony (measured by EEG). As a measure of moment-to-moment global phase synchrony we used a sliding window adaptation of the common phase-locking value (PLV; Lachaux et al. 1999) averaged across all channels. We found that fluctuations in PLV in the high-α frequency band (~10–12 Hz) over time correlated with activity (fMRI signal) in a specific set of bilateral parietal and frontal regions, comprising dorsolateral prefrontal cortex (dlPFC), rostro-lateral prefrontal cortex (rlPFC), inferior parietal cortex (IPL), and paracingulate cortex. This set of regions constituted the so-called FP network, derived from functional connectivity analyses of resting-state fMRI data (e.g., Dosenbach et al. 2007; Seeley et al. 2007; Cole et al. 2013) and activity-based imaging investigations (Dosenbach et al. 2006; Sadaghiani and D'Esposito 2015). The results were highly selective; α-band phase-locking did not correlate with any regions outside of the FP network, and activity in the FP network did not correlate with phase-locking in any other frequency band.

The FP network has been suggested to underlie phasic and adaptive aspects of executive control. Specifically, it is implicated in adaptive adjustments of cognitive and executive functions such as during initiation of control, in response to errors (Dosenbach et al. 2007), and during rapid set-switching (Seeley et al. 2007). The ability to switch between tasks or cognitive sets in particular is commonly conceptualized as cognitive flexibility (Scott 1962). Taking together the functional role of the FP network and the relation of its activity with α-band phase-locking, we have proposed that the FP network modulates α-band phase-locking across distant brain areas to implement phasic modulation of information exchange (Sadaghiani and Kleinschmidt 2016). In this view, top-down modulation of α-band phase locking is a neurophysiological mechanism for adaptive adjustment of long-range information exchange. This neurophysiological mechanism allows for efficient cognitive adjustments in response to changing top-down control demands, e.g., as needed during set-shifting. Consequently, according to this view reduced modulation of α-band phase locking would result in decreased cognitive flexibility.

Here, we tested the hypothesis that the FP network is necessary for the modulation of long-range phase locking in the high-α band (10–12 Hz). We furthermore hypothesized that this modulation is functionally important for tasks requiring cognitive flexibility. Lesion studies continue to provide a unique window into the necessity of specific brain structures for particular cognitive functions and their neural mechanisms (Rorden and Karnath 2004). More recently, the importance of lesion studies in understanding the function of large-scale networks identified on the basis of resting-state fMRI has been emphasized (Gratton et al. 2012; Adolphs 2016). Taking such a neuropsychological approach, we argue that if the FP network is necessary for the modulation of high-α band phase synchrony, then lesions to the FP network would disrupt this modulation. To this end, we measured EEG during resting wakefulness in patients with focal prefrontal lesions that overlapped with the FP network to varying degrees, as well as in healthy controls. We assessed the degree to which high-α-band phase synchrony is modulated as a function of lesion extent to the FP network. Furthermore, since α-band phase-locking modulation is functionally involved in cognitive flexibility (Pang et al. 2016), a core function of the FP network (Dosenbach et al. 2007), performance under such cognitive flexibility demands should decline in patients with lesions to the FP network.

Methods

Participants

Twenty-three patients with chronic focal lesions to the prefrontal cortex were recruited at the Department of Neurosurgery, Oslo University hospital—Rikshospitalet (Table 1; 11 women; ages 23–63 years, mean 46.2 ± 9; 9 bilateral, 6 right, and 8 left hemisphere lesions). Lesion etiology was low-grade gliomas ($n = 14$) or meningiomas that were resected on average 37.5 ± 28 (min 6) months prior to data collection. Inclusion criteria include a single lesion in frontal lobe and no other neurological or psychiatric disease or history of substance abuse. Patients were not selected based on lesion location within the prefrontal cortex. Instead, we hypothesized that the extent of lesion to the FP network would predict severity of disruption in α-band phase synchrony and in cognitive flexibility. Seventeen of the 23 lesion patients had some degree of lesion to the FP network. Accordingly, most analyses are based on % volume of the FP network (or % volume of bilateral dlPFC or rlPFC, respectively) that was lesioned. Thirteen healthy, age-matched subjects (8 women, ages 24–60 years, mean 44.6 ± 10.6) served as controls. All participants gave written informed consent according to procedures of the Norwegian Regional Committee for Medical and Health Research Ethics, South-East Norway. All participants underwent EEG, off-line resting-state fMRI, and structural MRI recordings.

EEG and MRI data acquisition

Continuous EEG-data was recorded during 5 min eyes-closed resting wakefulness from a 128-channel HydroCel Geodesic Sensor Net and Net Amps 300 amplifier (Electrical Geodesics, Eugene, OR) at a 250-Hz sampling rate. Impedance was kept below 100 Ω. Six electrodes were used to record eye movements and were excluded from subsequent spectral analyses. Conform with the PLV analyses by Lachaux et al. (1999) and our previous

Table 1 Patient demographics and % lesion (rounded to nearest half) of bilateral fronto-parietal (FP) network, bilateral dlPFC (node of FP network), bilateral rlPFC (node of FP network) and bilateral cingulo-opercular network (CO, for comparison). MG: Meningioma, LGG: Low-grade glioma, BA: Brodmann areas partially overlapping with the reconstructed lesion on the basis of the Brodmann map in MRIcron (Rorden and Brett 2000). Note that % lesion overlap values are in general relatively small as they are based on networks from seed-based functional connectivity that are expansive and also include structures outside the frontal lobe.

Patient	Lesion etiology	Months post-resection	Age	BA left	BA right	Lesion size (mm^3)	Lesion FP %	Lesion dlPFC %	Lesion rlPFC %	Lesion CO %
1	LGG	23	38	6,8,24,32	—	49 986	3	3	0	11.5
2	LGG	20	36	—	6,8,9,24,32,46	100 032	11.5	12.5	0.5	17.5
3	LGG	33	23	—	9–11,32,44–47	80 045	11.5	15	19	6
4	LGG	30	42	—	8,9,32,44–46	34 439	8	14	0	3.5
5	LGG	51	38	—	6,44,45	29 308	8	13	0	1.5
6	MG	13	52	10,11,47	10,11,32,46,47	69 053	3.5	0	34	0.5
7	LGG	27	41	4,6,9,44		24 796	9	14.5	0	0
8	LGG	68	55	—	4,6,8,9,32,44–46	60 058	18.5	31.5	0	2
9	MG	48.5	51	10,11,46,47	10,11,47	79 841	5	0	44	0
10	MG	13	45	10,11,47	10,11	39 731	2	0	14	0
11	MG	19	45	11	—	5051	0	0	0	0
12	MG	43	54	9–11,32,46,47	9–11,32,46,47	134 769	5.5	0	33	2.5
13	LGG	112	56	—	6,9,32,44–47	72 842	17.5	29.5	3	5
14	MG	27	48	11	11,47	7210	0	0	0	0
15	MG	44	53	10,11	—	2918	0	0	0	0
16	LGG	7	47	11,25	10,11,25	28 591	0	0	0	0
17	MG	52	61	—	9–11,32,46,47	48 730	3.5	0	27.5	1
18	LGG	31	41	45	—	771	0	0	0	0
19	LGG	9	42	6	—	10 141	0	0	0	1
20	LGG	54	45	9,10,32,45,47	—	25 023	3	3.5	6.5	6
21	LGG	6	36	6,8–11,24, 32,46,47	—	77 486	8.5	7	12.5	6.5
22	MG	20	63	10,11,24,25,32,47	—	96 762	2	0	16.5	2
23	LGG	104	51	3,4,6	—	42 796	3	5	0	0

study building the basis for the current investigations (Sadaghiani et al. 2012), recordings were re-referenced to a common average reference, and the original reference electrode was recalculated as FCz.

Whole-brain structural images were collected on a whole-body Philips Achieva 3-T scanner with an 8-channel Philips SENSE head coil (Philips Medical System, Best, The Netherlands). A combination of T1 and T2 weighted images were recorded. Anatomical images were acquired using a T1-wighted Turbo Field Echo (TFE) pulse sequence (Repetition time [TR]: 6.5 ms, Echo time [TE]: 3.1 ms, Flip angle 8 degrees. 170 sagittal slices; field of view [FOW] = 256 × 256 × 204 mm, voxel size 1 × 1 × 1 mm). Additionally, a T2-weighted FLAIR image was recorded to aid lesion detection (Repetition time [TR]: 4800 ms, Echo time [TE]: 305 ms, Flip angle 90 degrees. 170 sagittal slices; field of view [FOW] = 256 × 256 mm, voxel size 1 × 1 × 2 mm).

Structural volume of interest and lesion assessment

FP network volume of interest: The location of the FP network was based on our previous study (Sadaghiani et al. 2012). Note that using an independent dataset (rather than the current healthy controls) for network definition ascertained an unbiased comparison between the patient and control groups. As described in detail in Sadaghiani et al. (2012), the FP network was defined by seed-based intrinsic functional connectivity fMRI analysis. The spherical seeds (6-mm radius) were centered on left and right dlPFC at standardized stereotactic coordinates [x y z] = ±43, 22, 34 (Dosenbach et al. 2007). The time-course for all subject-specific gray-matter voxels in the 2 spheres were averaged to form a regressor for a general linear model. The group-level statistical map from 26 participants corresponding to this regressor was then thresholded at FWE $P < 0.01$ to yield the FP network mask. This procedure also yielded masks for individual nodes of the FP network bilaterally including dorsolateral prefrontal cortex (dlPFC), rostro-lateral prefrontal cortex (rlPFC), paracingulate cortex, and inferior parietal cortex (IPL).

Network lesion assessment: Lesion masks were traced manually in native patient space according to visible damage on a T1-weighted anatomical scan and guided by damage and hyper-intensities on a T2-weighted FLAIR image and examined for anatomical specificity by a neurologist (R.T.K.). For each patient, the amount of damage to the FP network was quantified by counting the voxels in the network mask (reverse normalized to the individual patient's native space) that overlapped with the lesion mask, divided by the total number of FP network voxels (Nomura et al. 2010). The absolute number of voxels in the spatially normalized lesion mask served as a control variable accounting for differences in lesion size. Approximate correspondence of regions and lesions to Brodmann areas (BA) was assessed using the Brodmann map provided in MRIcron (Rorden and Brett 2000). These rough correspondences should be interpreted with care due to imprecision of BA maps in humans.

EEG analysis

Preprocessing: We used the Fieldtrip MATLAB toolbox (Oostenveld et al. 2010). Power line noise was removed by band-stop (notch) filtering at 50 Hz. The signal was band-pass filtered between 0.5 Hz and 70 Hz. EEG channels with unusually low signal-to-noise ratio were visually identified and excluded from subsequent analyses (controls mean = 9.6, range 6–17; all patients mean =

10.3, range 6–27; dlPFC patient subgroup: mean = 7.8, range = 6–9; rlPFC patient subgroup: mean = 13, range = 6–27). Independent component analysis (ICA) was used to remove eye, muscle, and heart artifacts by visually identifying the respective artifact components from their topography, time-course, and kurtosis and frequency spectrum thereof.

Phase-Locking modulation: The procedure summarized in Figure 1 was performed using custom code in MATLAB (available at github.com/SepidehSadaghiani/PLV_modulation.git). We calculated phase-synchrony over time to measure its spontaneous continuous modulations. PLV time-courses were obtained in accordance to procedure in Sadaghiani et al. (2012). In particular, data were first band-pass filtered to the high-α band (10–12 Hz). The order of the finite–impulse–response band-pass filter was chosen to cover 4 cycles of the frequency band. To calculate PLVs continuously over time rather than across trial repetitions, the formula introduced by Lachaux et al. (1999) was adapted as follows:

$$PLV = \frac{1}{N}\left|\sum_{n=1}^{N} e^{i(\Phi_{chn1(n)} - \Phi_{chn2(n)})}\right|$$

where *N*=number of time points in a time window. We used the Hilbert transformation to calculate the analytic phase at time point *n* for channel *x* as $\phi_{chn\_x}(n) = \arctan(u(n)/v(n))$, where *v* is the real part of the analytic signal and *u* is the Hilbert transform or the imaginary part of the analytic signal. |.| represents the complex modulus. For a given channel pair, the difference in phase was calculated at each time point. PLV was calculated within a 10-s window sliding in 2 s steps and hence resulting in a PLV time-course sampled at 0.5 Hz. Each PLV value reflects the consistency of phase lag between 2 channels across 10 s. The PLV time-course was then averaged across all channel-pairs resulting in a global PLV time-course.

Moment-to-moment differences in power may affect the reliability of phase estimations. This issue was not critical in our previous paper that assessed co-variability of phase locking with the fMRI BOLD signal and would at most have resulted in false negatives (Sadaghiani et al. 2012). However, it may be critical and result in spurious modulation in the current study that is interested directly in the moment-to-moment variability of phase locking. Therefore, here the global PLV time-course of each canonical band was normalized to the mean of the PLV time-courses of all frequency bands. Paralleling the commonly used calculation of *relative* power (Kropotov 2009), the resulting *relative* PLV is expected to be more robust against moment-to-moment fluctuations in signal-to-noise ratio that affect PLV estimability across the full frequency spectrum. Furthermore,

this relative measure allows a more selective assessment of effects in the α band over and above changes occurring across the full spectrum.

Our central interest in this study was to assess modulation of phase locking over time. As 2 measures of signal time-course modulation, we calculated range (maximum–minimum) and standard deviation (STD) of the relative global PLV time-courses.

Band-pass filtering, PLV time-course calculation and assessment of its modulation were performed for high-α (10–12 Hz), and repeated for each of the control frequency bands δ (1–3 Hz), θ (4–7 Hz), low α (8–10 Hz), β (13–25 Hz), γ (26–45 Hz). Note that in contrast to Sadaghiani et al. (2012), we did not determine the high-α band individually in the current study, as the α peak frequency itself might have shifted due to lesion.

Power modulation: As a control, we quantified modulation of relative power. A time–frequency analysis at 2-s temporal resolution, 50% window overlap and frequency resolution of 0.25 Hz was performed using the multitaper approach in Fieldtrip. Spectral power in the high-α band was averaged across all electrodes, and this global field power time-course was divided by the mean global field power across all canonical frequency bands to generate *relative* power. Finally, range and STD of this relative high-α band power time-course was assessed.

As an alternative approach, we assessed magnitude modulation directly from the analytic signal underlying the PLV calculation. Analytic amplitude (i.e., envelope) at each time point *n* is defined as the absolute value of the analytic signal, i.e., $\sqrt{u(n)^2 + v(n)^2}$. To parallel the PLV analysis, the amplitude time-course was resampled to 0.5 Hz resolution (2 s steps), averaged across all electrodes, and normalized to the mean of the amplitude time-courses of all frequency bands. Range and STD of this relative high-α band amplitude time-course was assessed.

Neuropsychological testing

To assess the behavioral relevance of α-band phase-locking modulation, we investigated the cognitive set-shifting condition of the Trail-Making Test (TMT) from the Delis–Kaplan Executive Function System (D-KEFS; Delis et al. 2001) designed to measure cognitive flexibility (Kortte et al. 2002; Lezak 2004). No other behavioral measures beyond this hypothesis-driven choice were investigated in this study in order to avoid the issue of performing multiple statistical comparisons. The TMT requires connecting ordered elements such as numbers and letters in the correct sequence as fast and accurately as possible. The D-KEFS implementation used here (Delis et al. 2001)
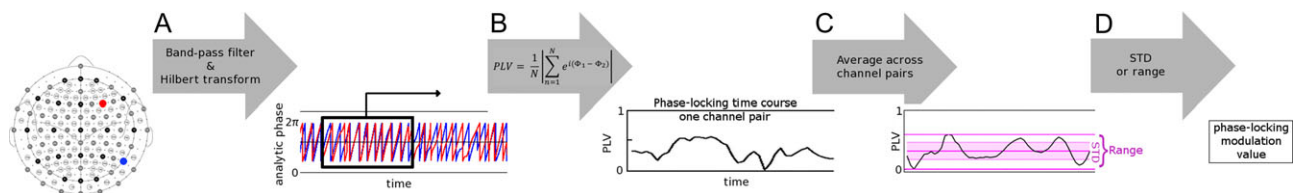

Figure 1. Calculating modulation in band-limited phase synchrony. (A) The analytic phase is assessed for each channel and time point by applying the Hilbert transformation on band-filtered signal time-courses. For a given pair of channels (marked by red and blue circles), the difference in analytic phase is calculated at each time point. (B) This phase difference is averaged across N time points within a time window of 10 s (black rectangle) that is sliding over time at 2 s intervals. The amplitude (|.|) of this averaged difference is the phase-locking value (PLV). PLV measures the consistency of phase lag between the 2 channels over the course of 10 s (Sadaghiani et al. 2012). (C) PLV time-courses were averaged across all channel-pairs resulting in a global PLV time-course. This time-course was normalized to PLV across all other frequency bands (relative PLV). (D) PLV modulation strength was assessed as standard deviation (STD) and range (maximum–minimum) of the relative global PLV time-course.

consists of 5 pen and paper tasks, each with stimuli spread over an 11 × 17-inch area: visual scanning (TMT1), number sequencing (TMT2), letter sequencing (TMT3), number-letter switching (TMT4), and motor speed conditions (TMT5). In the visual scanning condition, subjects hooked off all 3 s on the response sheet. In the number sequencing condition, subjects drew a line between the numbers 1 through 16 in order while ignoring letters on the response sheet. In the Letter sequencing condition, subjects connected the letters A through P in alphabetic order while ignoring numbers on the sheet. In the number-letter switching condition, subjects switched back and forth between connecting numbers and letters (1-A-2-B-3-C-… 16-P). Finally, in the motor speed condition subjects traced over a dotted line along a path between circles as quickly as possible, allowing to measure their motor drawing speed. There is a short practice trial prior to each condition. Participants are instructed to complete all tasks as quickly and as accurately as possible. According to D-KEFS TMT procedures, completion time for each of the 5 conditions was measured by a stopwatch. We focused on the set-shifting condition (Condition 4) in order to investigate cognitive flexibility. Raw scores of time-on-task were transformed into standardized scores in following D-KEFS scoring procedures on the basis of US age-adjusted normative data (normative mean = 10, SD = 3) (Delis et al. 2001). Raw (sec) as well as standardized scores are provided in Supplementary Table S1. Standardized scores of time to complete the switching condition were investigated as a function of α-PLV modulation across subjects and compared between lesion groups and healthy controls.

Results

We hypothesized that the extent of lesion to the FP network predicts the severity of disruption in α-band phase-synchrony modulation. To test this hypothesis, the location of FP network from our previous study was used (Sadaghiani et al. 2012). This seed-based fMRI connectivity map bilaterally comprised dlPFC, rlPFC, IPL, and paracingulate cortex (Fig. 2B. The network's 3D volume can be accessed at https://neurovault.org/collections/3881/). For each frontal lobe patient, we assessed the percentage of FP network volume that was lesioned (example in

Fig. 2C,D). Percent lesion overlap for all patients is presented alongside patient demographics in Table 1.

We calculated PLV over time in a sliding window procedure for the high-α band and several canonical frequency bands as controls (cf. Sadaghiani et al. 2012). Modulation of these time-courses was calculated using range (maximum–minimum) and STD (Fig. 1). We then assessed the relation between phase-locking modulation, brain lesion, and task performance. We report both power and phase locking as *relative* measures to account for moment-to-moment fluctuations in signal-to-noise ratio affecting the full frequency spectrum. All regressions are corrected for overall lesion size and age. Effects where direction was clearly hypothesized based on our prior work are reported as one-sided tests. All additional tests are explicitly indicated as two-sided.

Modulation in phase synchrony as a function of brain lesion

As hypothesized, lesions to the FP network diminished modulation in the α-band global phase locking (Fig. 3A). Across all patients, the range ($r^2 = 0.25$, $P < 0.05$) as well as STD ($r^2 = 0.25$, $P < 0.05$) of relative high-α band phase locking decreased as a function of % lesion to the FP network (Fig. 3A). Splitting patients by median FP lesion extent showed a significant difference in high-α PLV modulation between severe and low FP lesion groups ($t_{21} = 1.9$, $P < 0.05$). FP network lesion had no significant impact on PLV modulation in any other frequency band, confirming the spectral specificity of our effects (range δ: $P = 0.29$; θ: $P = 0.66$; low α: $P = 0.30$; β: $P = 0.20$, γ: $P = 0.6$, and STD δ: $P = 0.12$; θ: $P = 0.84$; low α: $P = 0.40$; β: $P = 0.37$, γ: $P = 0.83$, all two-sided). We further observed evidence for a key role of the dlPFC node of the FP network. The 2 patients with highest FP network damage and low high-α band PLV modulation (Subjects 8 and 13 in Fig. 3A) had lesions that covered the dlPFC particularly well (lesion map in Fig. 4A,B). Consequently, we performed an additional regression using % lesion to dlPFC in patients with at least 1% lesion to this node (Fig. 3B. These patients are highlighted in Fig. 3A by filled circles). Again, relative high-α-band phase-locking modulation decreased with increasing lesion size and showed a stronger relationship than
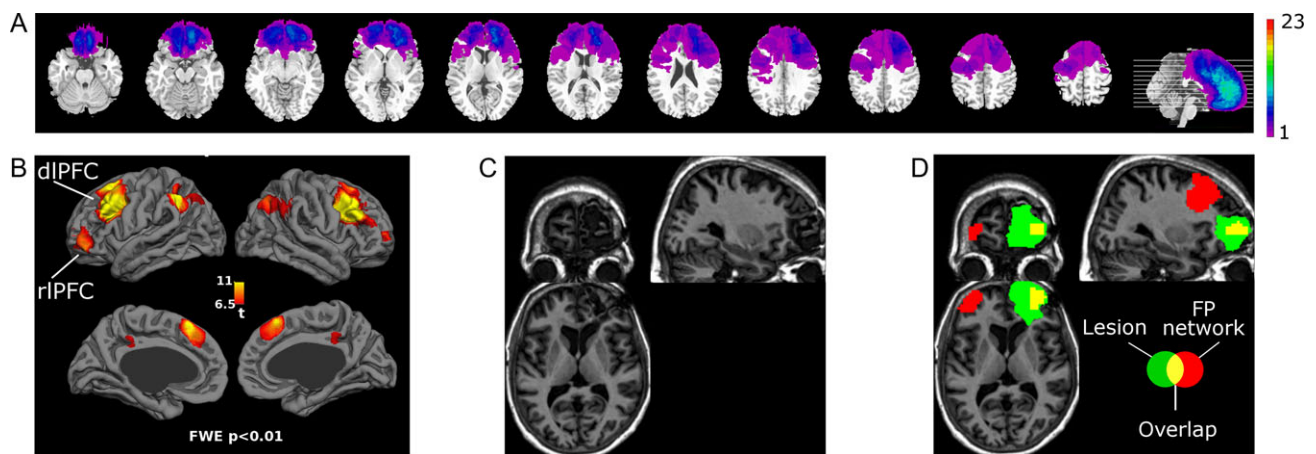

Figure 2. (A) Voxel-wise overlap of lesion across all 23 patients. Scale indicates number of patients with lesion in a given voxel. (B) Fronto-parietal (FP) network defined using resting-state fMRI in an independent pool of 26 healthy participants (Sadaghiani et al. 2012). (C) Structural image showing lesion in a single patient (subject 17) with lesion to right rlPFC node of the FP network. (D) Overlap of this patient's lesion with the FP network, demonstrating assessment of % lesion to the FP network.
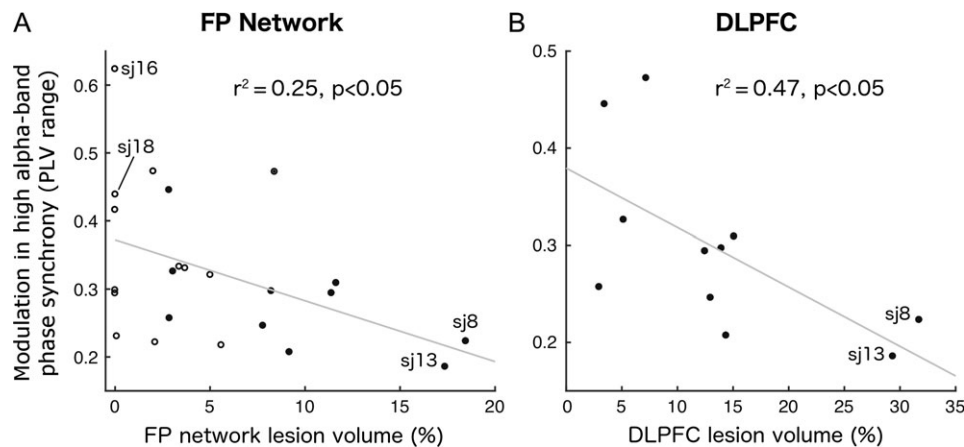
Figure 3. The impact of lesion on phase-synchrony modulation. (A) Modulation of relative high-α phase synchrony as a function of FP network lesion volume. (B) Strong modulation of relative high-α-band phase synchrony as a function of dlPFC volume (as percentage of left and right dlPFC combined) lesioned in patients with dlPFC damage. For comparison, these patients are marked by filled circles in A. Subject labels mark the 2 patients with the highest FP network lesion and weak phase-synchrony modulation (sj8 and sj13) as well as the 2 patients with lowest FP network lesion in combination with strong phase-synchrony modulation (sj16 and sj18). Lesion maps for these 4 patients are shown in Fig. 4.

with overall FP lesion (Fig. 3B, range $r^2 = 0.47$, $P < 0.05$, STD $r^2 = 0.44$, $P = 0.051$).

To control for anatomical specificity, we investigated another network with frontal nodes associated with cognitive control functions called the cingulo-opercular network (CO, Fig. 5. The network's 3D volume can be accessed at https://neurovault.org/collections/3880) with a comparable range of lesion overlap (0.5–17.5% compared to 2–18.5% in the FP network). In this network, % lesion did not correlate with high-α-band PLV range ($r^2 = 0.11$, $P = 0.75$) or STD ($r^2 = 0.11$, $P = 0.91$).

To further investigated the potential dominance of the dlPFC in the relationship to high-α band phase-synchrony modulation, we directly compared lesion impact from this node to that of another frontal node of the FP network denoted rlPFC (Fig. 6). To this end, the 17 patients with lesions to the FP network were subdivided into subgroups with predominant dlPFC node ($n = 8$) versus rlPFC node ($n = 9$) lesions. These subgroups were comparable in the percentage of the lesion that comprised the respective node ($t_{15} = 1.37$, $P = 0.19$, mean lesions: dlPFC = 15.37%, and rlPFC = 22.97%), overall lesion size ($t_{15} = 1.44$, $P = 0.17$), and age ($t_{15} = 0.61$, $P = 0.55$). We found a significant reduction in PLV modulation in the dlPFC lesion subgroup versus the rlPFC lesion subgroup (range $t_{15} = 2.42$, STD $t_{15} = 2.30$, $P < 0.05$, two-sided). As hypothesized, we also found a decrease in PLV modulation in patients with more dlPFC lesions versus healthy controls (range $t_{19} = 1.71$, STD $t_{19} = 1.73$, $P = 0.05$. Age was matched: $t_{19} = 0$). No difference was observed between the rlPFC subgroup and healthy controls ($t_{20} = 0.15$). These findings speak to the necessity of an intact dlPFC for modulation of phase synchrony in the high-α band, while no such effect was observed for rlPFC.

Controlling for oscillation power and power modulation

To exclude a potential spurious contribution of signal strength stemming from volume conductance in scalp EEG, we performed analogous analyses on high-α power. FP network and dlPFC lesion extent did not correlate with modulation in relative power of high-α oscillations (FP network range: $P = 0.13$, STD: $P = 0.24$; dlPFC range: $P = 0.72$, STD: $P = 0.78$, two-sided). Alternatively, assessing signal strength directly as amplitude (i.e., envelope) of the analytic signal that PLV was derived from

expectedly confirmed absence of magnitude effects (FP network range: $P = 0.12$, STD: $P = 0.22$; dlPFC range: $P = 0.90$, STD: $P = 1$, two-sided). These findings indicate that the phase synchrony we measured did not arise from a single oscillatory source projecting onto different electrodes, and furthermore that the effects we observed were not driven by the dependence of phase estimation reliability on signal power. Similarly, the dlPFC lesion, rlFPC lesion and healthy control groups (cf. Fig. 6) did not show differences in the range or STD of high-α oscillation power (all pairwise comparisons for range and STD $P > 0.28$, two-sided). Likewise, *mean* PLV did not correlate with FP network lesion ($P = 0.62$), supporting the view that the FP network modulates high α band phase synchrony rather than being involved in its generation. Finally, the relationships presented in Fig. 3A and B maintained strong effect sizes after excluding the 43 electrodes over frontal cortex ($r^2 = 0.28$, and $r^2 = 0.53$ $P < 0.05$), indicating that the reduction in α-band PLV modulation was not simply due to loss of α-band signal from brain volume loss.

Behavioral performance as a function of brain lesion and modulation in phase synchrony

Next, we investigated the dependence of cognitive flexibility, a core function of the FP network, on high-α-band phase-locking modulation using the TMT (Delis et al. 2001). This common neuropsychological test assesses cognitive flexibility in a set-shifting condition, while controlling for visual scanning and motor speed. While we did not find a correlation between lesion extent and task performance (FP network lesion (all 23 patients): $P = 0.37$; dlPFC lesion ($n = 11$ with dlPFC lesion): $P = 0.45$, two-sided), performance differed significantly between lesion groups and healthy controls. Paralleling the above-described group differences in PLV signatures (cf. Fig. 6), behavioral performance was significantly deteriorated in patients with dlPFC lesions compared to healthy controls ($t_{19} = 4.2$, $P < 0.0005$) and patients with rlPFC lesions ($t_{15} = 2.28$, $P < 0.05$) (Fig. 7). The latter group did not differ from healthy controls ($t_{20} = 1.0$, $P = 0.33$ two-sided). This effect was specific to the set-shifting condition whose standardized score is corrected for effects in other task conditions, but absent in the other 4 conditions of the task designed to measure stimulus set-maintenance,
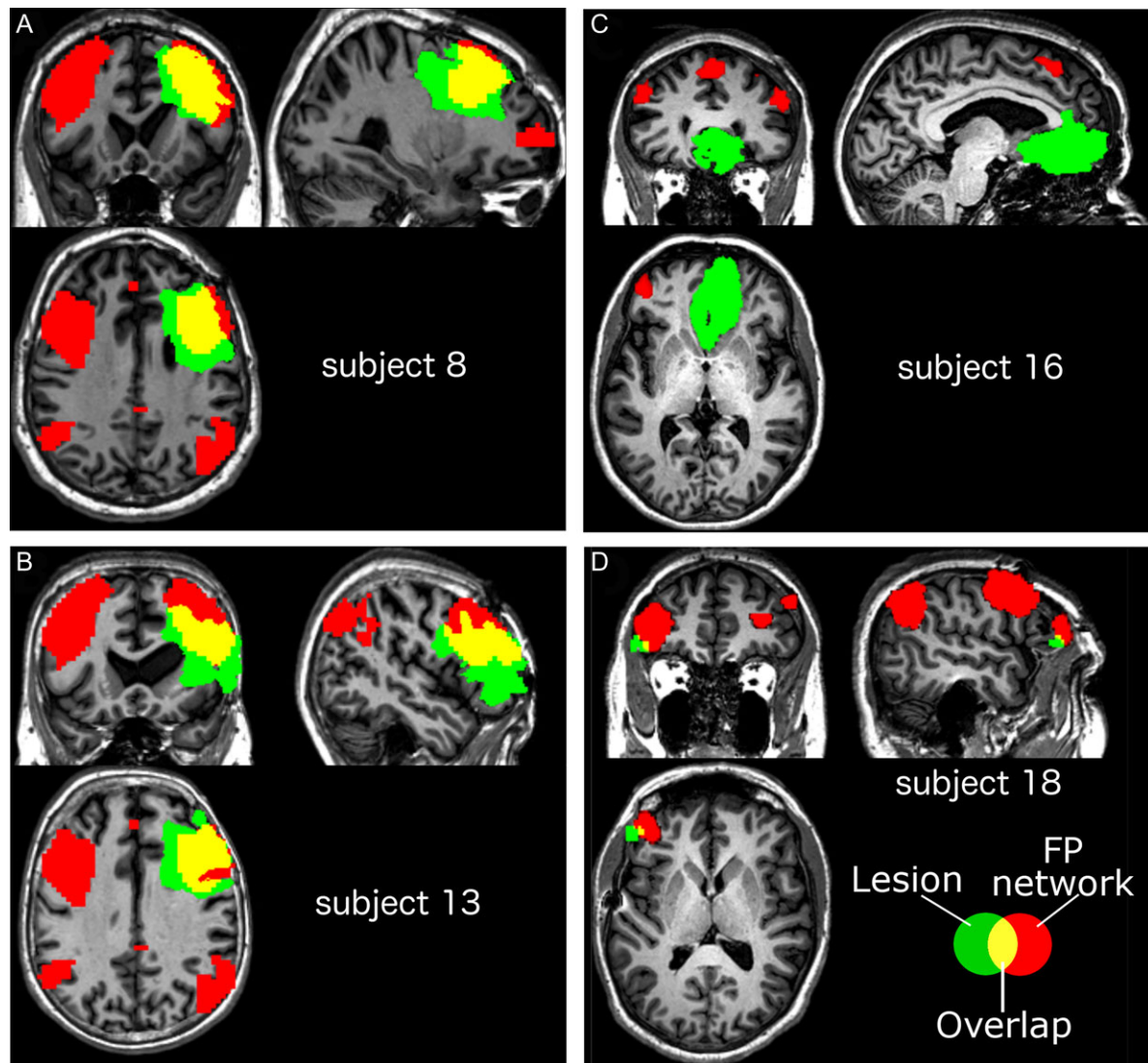
Figure 4. Comparing degree of overlap between lesions and the FP network. A and B show the 2 patients with the highest FP network lesion and weak phase-synchrony synchrony modulation (cf. Fig. 3A,B). These patients have focal lesions particularly well overlapping with the dlPFC node of the FP network (31.5% and 29.5% of the combined left and right dlPFC volume damaged, respectively). For comparison, Panels C and D show the 2 subjects with lowest FP network lesion in combination strong phase-synchrony modulation (cf. Fig. 3A). Lesion in these patients has no overlap with the dlPFC. Subject 16 has lesion to the ventromedial prefrontal cortex, while Subject 18 has a lesion bordering the rlPFC (0.1% overlap).

visual scanning and motor speed but lacking cognitive flexibility demands (all pairwise group comparisons $P > 0.17$, two-sided).

Investigating the direct correlation between high-α-band PLV modulation and set-shifting performance across all patients and healthy controls revealed a significant relationship. However, an equivalent control analysis with high-α-band *power* also showed a significant correlation with behavior, rendering the interpretation of phase-locking data ambiguous since power differences can compromise PLV metrics. Full details of this analysis are provided in Supplementary data.

Discussion

The FP network is known to support cognitive flexibility (Seeley et al. 2007; Cole et al. 2013), and exhibits activity fluctuations correlated with changes in high-α band phase synchrony (Sadaghiani et al. 2012). Based on our previous work, we

hypothesized that lesions to the FP network result in a reduction in the modulation of long-range phase locking in the high-α band (Sadaghiani and Kleinschmidt 2016). Here, we confirmed this prediction in a group of patients with focal frontal lobe resections. The extent of lesion to the FP network, but not overall lesion size or lesion to another higher-order network with frontal nodes (i.e., cingulo-opercular), disrupted phase-locking modulation in the high-α band. This finding provides evidence for the functional necessity of the FP network—most notably its dlPFC node—for modulatory control of α band long-range phase synchrony. Furthermore, based on the central role of the FP network in adaptive aspects of cognitive control (Dosenbach et al. 2007), we hypothesized that this reduction in modulation of high-α band phase locking would result in disruption of behavioral performance when cognitive flexibility is needed. Indeed, we found a significant reduction of performance on the TMT during the set-shifting condition, but not in other non-
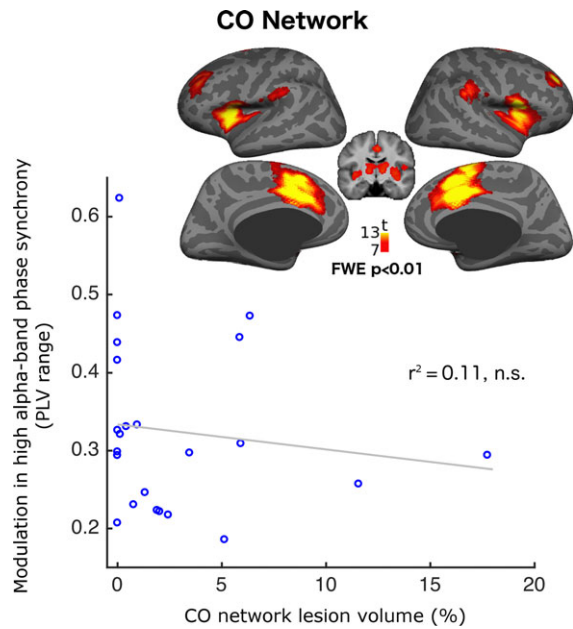
CO Network

Figure 5. Demonstrating absence of impact of cingulo-opercular (CO) network lesion on phase-synchrony modulation. The graph shows modulation of relative high-α phase synchrony as a function of CO network lesion volume. The brain map shows the CO network defined using resting-state fMRI in an independent pool of 26 healthy participants (Sadaghiani et al. 2010).
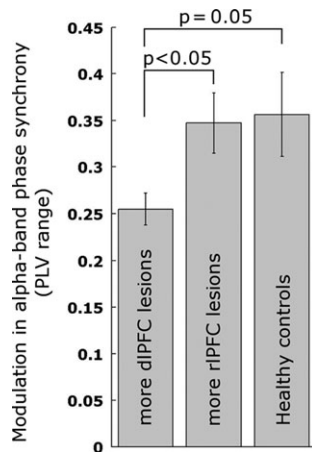

Figure 6. Modulation in relative α-band phase synchrony depends on dlPFC but not rlPFC node of the FP network. Error bars show ± standard error.

executive conditions, in patients with lesions to the dlPFC, a core node of the FP network.

Special role of the dlPFC

The strongest reduction in α-band phase-locking modulation and disruption of cognitive flexibility was observed in patients with lesions to the dlPFC node of the FP network. While our previous simultaneous EEG-fMRI study found significant co-variation of high-α band phase synchrony and BOLD activity in *all* regions of the FP network (Sadaghiani et al. 2012), the current findings indicate that not all regions of the network are *necessary* for enabling modulatory impact onto α band phase
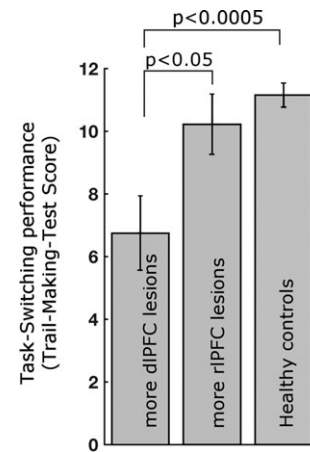

Figure 7. Cognitive set-shifting performance depends on dlPFC of the FP network. No impact was observed for the rlPFC node. Standardized score of the Trail-Making Test Number-Letter switching condition. Error bars show ± standard error.

locking. Specifically, while we found evidence in support of necessity for the dlPFC, lesion to the rlPFC node of the network had no impact on our EEG measure. This dissociation highlights the strength of lesion studies to complement functional imaging studies. Although we cannot conclude that the dlPFC is the causal initiator of α phase synchrony modulation, our lesion approach provides support for this region as a necessary component of the causal chain of neuronal events. Functional MRI studies contrasting set-switching versus monotonous control conditions of the Trail-Making Test have found (left hemispheric) dlPFC activation with peak coordinates overlapping with the dlPFC node used in the current study ((Moll et al. 2002; Zakzanis et al., 2005); for a recent review see (Varjacic et al. 2018)). Lesion studies of Trail-Making Test set-shifting performance further report behavioral impairment in frontal lobe lesion patients as compared to non-frontal lesions, and within the frontal lobe most markedly in dorsolateral areas ((Stuss et al. 2001; Yochim et al. 2007), with the latter study providing a lesion map supporting direct overlap with the dlPFC node used in the current study). These observations together support a strong role of the dlPFC in generating modulatory top-down control signals. However, our study population was limited to lesions in the frontal lobe and we therefore could not directly investigate and compare the role of parietal nodes of the FP network. Future studies with more comprehensive patient pools are necessary to investigate this question. Yet, when compared to the lesion impact from another, more rostrally situated frontal node of the FP network denoted rlPFC, the dlPFC appeared to maintain a special role in controlling high-α band phase synchrony and cognitive flexibility.

Cognitive function of high-α band phase synchrony and the possible underlying mechanism

Cognitive control networks such as the FP network are postulated to be involved in top-down modulation of information processing across dynamic task-relevant sensory and motor ensembles. To this end, top-down signals originating in lateral PFC (such as signals representing current task goals) may implement cognitive control by biasing information flow across such task-relevant neural ensembles (Miller and Cohen 2001). The mechanisms for such targeted bias in information flow are

currently largely unknown. It has been suggested that synchronization of α band oscillatory activity across distant regions facilitates information flow between these regions (Palva and Palva 2011). This view is supported by enhanced performance under increased α band phase synchrony (von Stein and Sarnthein 2000; Mima et al. 2001; Sauseng et al. 2005; Doesburg et al. 2009; Palva et al. 2010; Zanto et al. 2011). We have suggested that the FP network modulates this cross-regional α-band phase synchrony to bias information flow according to dynamically shifting processing demands (Sadaghiani and Kleinschmidt 2016). This oscillatory mechanism provides a possible neurophysiological underpinning for the function of the FP network in phasic and adaptive cognitive control. Our results support this view by showing that modulation of α-band phase synchrony depends on intact FP network, especially the dlPFC, and is linked to cognitive flexibility as measured with TMT set-shifting performance.

Assessing neurophysiological markers at resting state

The observed relation between resting phase-locking modulation of α-band phase synchrony and behavior (Fig. 7) supports the view that behaviorally relevant physiological markers can be measured at resting state. We interpret phase-locking modulation at resting state as a measure of "neural flexibility" that can manifest as cognitive flexibility under task demands. In line with this view, numerous previous studies have observed that resting-state oscillatory activity correlates with behavior. Regarding α-band oscillations in particular, it has been reported that their amplitude characteristics during resting state predict performance on a variety of tasks in healthy participants (Smit et al. 2013) and their amplitude and phase synchrony correlate with cognitive symptoms in various clinical conditions (Sponheim et al. 2000; Allen et al. 2004; Kwak 2006; Dubovik et al. 2012; Woltering et al. 2012). Here, we introduced *modulation* in resting-state EEG measures as a new marker and proved its informativeness, much like the introduction of sliding window-based measures to access *dynamic* functional connectivity in fMRI (Preti et al., 2017; Kucyi et al. 2018). To further refine functional understanding of the temporal and spatial aspects of α-band phase synchrony, our current findings motivate and call for future studies investigating phase-locking modulation under various levels of phasic adaptive control demands during tasks. Supporting the convergence across task-based and resting-state neurophysiological markers, a magnetoencephalography study found increased phase synchrony selectively in the α-band across task-relevant occipital cortices and the rest of the brain during dimensional set-shifting in healthy participants (Pang et al. 2016).

Limitations

Electrical leakage is an inherent concern in EEG-based investigations of phase synchrony. One suggestion to mitigate this issue is to discard all phase synchrony that has no phase lag and may hence stem from a single oscillatory source rather than multiple communicating neural populations. This is achieved by using the imaginary part of phase synchrony only (Nolte et al. 2004). A disadvantage of this approach is that potentially true phase synchrony may be discarded. In the current study we used the full PLV in line with our previous EEG-fMRI work (Sadaghiani et al. 2012). However, while our previous

work demonstrated that effects qualitatively persisted for *imaginary* PLV, the relationship between FP lesion and PLV in the current study did not survive restriction to imaginary. This is likely due to the limited sample size inherent to lesion studies requiring homogenous etiology (Adolphs 2016), as well as the heterogeneity of brain lesion locations (Rorden and Karnath 2004). We are further subject to the limitation that lesions do not abide to boundaries of functional regions (Rorden and Karnath 2004), thus leaving us with the likely simplistic use of models of linear relationships between *partial* lesions, EEG changes and cognitive disruptions. To confirm our observations using imaginary PLV, future lesion studies with higher power are needed. Importantly however, in our earlier EEG-fMRI study, retaining zero-lag PLV markedly strengthened effect size without changing spatial structure of the results (i.e., specificity to FP network). This indicates that the zero-lag proportion of our α-band PLV sliding window measure contained true phase synchrony. In that study, we further argued that spurious PLV modulation stemming from a single source should also appear as power modulation of the putative source. Contrary to this possibility, while α-band PLV modulation correlated with FP network fMRI activity, α-band power modulation mapped onto another anatomically non-overlapping brain network (CO network). In the current study, we followed the same logic to address volume conductance. We demonstrated that relative α-band power did not show significant correlation with FP network or dlPFC lesion extent, speaking for independence of PLV observations from power and volume conductance.

Further, while our main goal was to establish the necessity of FP network regions in modulating α-band phase synchrony, the additional demonstration of a direct link of our EEG measure to behavior faced several limitations. First, for this supplementary analysis it could not be ruled out that α-band power fluctuations contributed to phase-synchrony modulation measures via volume conductance. Second, while we found a significant phase synchrony-to-behavior relationship in healthy controls, there was only a trend in patients (see Supplementary materials). A likely reason for the reduced relationship in patients is a flooring effect of our phase synchrony measure in dlPFC lesion patients, in turn a result of signal-to-noise limitations of connectivity measured from surface EEG (cf. Supplementary Fig. S1A, where the lowest performance scores are not accompanied by further drop in phase-synchrony modulation as expected according to the linear fit, likely because noise alone causes a minimal amount of phase-synchrony modulation). Another potential limitation stems from the behavioral measure itself. Cognitive control functions such as cognitive flexibility are inherently difficult to measure in isolation, as any task inevitably co-engages multiple control functions as well as task-specific non-executive processes. Such task impurity (Miyake et al., 2000) may have additionally contributed to our finding that while cognitive set-switching performance differed significantly across dlPFC lesion, rlPFC lesion, and healthy groups, we did not observe a graded correlation between dlPFC lesion extent and behavior. Since we found a graded correlation for phase-synchrony modulation, it is likely that the latter is a better measure of cognitive functioning than performance on a single task. This possibility is exciting from a clinical point of view. EEG (especially a short resting state recording as in the current study) can be readily acquired in many neurological patient services and could complement extensive and expensive neuropsychological assessments to characterize cognitive

dysfunction and recovery. To corroborate this potential, future lesion EEG studies with more extensive behavioral batteries are required to permit isolation of a more pure cognitive flexibility measure in a factor analysis (Friedman and Miyake 2017).

Conclusions

This study demonstrates the informativeness of measuring *changes* in EEG-based resting-state markers of functional connectivity across time, e.g., by using sliding window procedures (Betzel et al. 2012). This approach can to some degree be compared to recently advanced fMRI-based dynamic functional connectivity measures (Preti et al. 2017). Enacting this approach, our observations suggest that phase-synchrony modulation in the high α-band at resting state depends on intact FP network, more specifically the dlPFC node. Moreover, dlPFC lesions cause reduced cognitive flexibility as measured by set-shifting. Our observations support the hypothesized causal link between the FP network, high α-band phase synchrony, and cognitive flexibility.

Supplementary Material

Supplementary material is available at *Cerebral Cortex* online.

Funding

Notes

References

Adolphs R. 2016. Human lesion studies in the 21st Century. Neuron. 90(6):1151–1153.

Allen JJ, Urry HL, Hitt SK, Coan JA. 2004. The stability of resting frontal electroencephalographic asymmetry in depression. Psychophysiology. 41(2):269–280.

Betzel RF, Abell M, O'Donnell BF, Hetrick WP, Sporns O. 2012. Synchronization dynamics and evidence for a repertoire of network states in resting EEG. Front Comput Neurosci. 6:74.

Cole MW, Reynolds JR, Power JD, Repovs G, Anticevic A, Braver TS. 2013. Multi-task connectivity reveals flexible hubs for adaptive task control. Nat Neurosci. 16(9):1348–1355.

Delis DC, Kaplan E, Kramer J. 2001. The Delis-Kaplan Executive Function System. San Antonio, TX: Psychological Corporation.

Doesburg SM, Green JJ, McDonald JJ, Ward LM. 2009. From local inhibition to long-range integration: a functional dissociation of alpha-band synchronization across cortical scales in visuospatial attention. Brain Res. 1303:97–110.

Dosenbach NU, Fair DA, Miezin FM, Cohen AL, Wenger KK, Dosenbach RA, Fox MD, Snyder AZ, Vincent JL, Raichle ME, et al. 2007. Distinct brain networks for adaptive and stable task control in humans. Proc Natl Acad Sci USA. 104(26): 11073–11078.

Dosenbach NU, Visscher KM, Palmer ED, Miezin FM, Wenger KK, Kang HC, Burgund ED, Grimes AL, Schlaggar BL, Petersen SE. 2006. A core system for the implementation of task sets. Neuron. 50(5):799–812.

Dubovik S, Pignat JM, Ptak R, Aboulafia T, Allet L, Gillabert N, Magnin C, Albert F, Momjian-Mayor I, Nahum L, et al. 2012. The behavioral significance of coherent resting-state oscillations after stroke. Neuroimage. 61(1):249–257.

Friedman NP, Miyake A. 2017. Unity and diversity of executive functions: individual differences as a window on cognitive structure. Cortex. 86:186–204.

Gratton C, Nomura EM, Pérez F, D'Esposito M. 2012. Focal brain lesions to critical locations cause widespread disruption of the modular organization of the brain. J Cogn Neurosci. 24(6):1275–1285.

Haegens S, Nácher V, Luna R, Romo R, Jensen O. 2011. α-Oscillations in the monkey sensorimotor network influence discrimination performance by rhythmical inhibition of neuronal spiking. Proceedings of the National Academy of Sciences. 108(48):19377–19382.

Klimesch W, Sauseng P, Hanslmayr S. 2007. EEG alpha oscillations: the inhibition-timing hypothesis. Brain Res Rev. 53(1): 63–88.

Kortte KB, Horner MD, Windham WK. 2002. The trail making test, Part B: cognitive flexibility or ability to maintain set? Appl Neuropsychol. 9(2):106–109.

Kropotov J. 2009. Quantitative EEG, Event-Related Potentials and Neurotherapy. Academic Press. http://www.electroneurodiagnostics.org/resources/EEG-Books/Quantitative-EEG—Event-Related-Potentials.pdf.

Kucyi A, Tambini A, Sadaghiani S, Keilholz S, Cohen JR. 2018. Spontaneous Cognitive Processes and the Behavioral validation of time-varying brain connectivity. Netw Neurosci. 2: 397–417.

Kwak Y. 2006. Quantitative EEG Findings in different stages of Alzheimer's disease. J Clin Neurophysiol. 23(5):457–462.

Lachaux J-P, Rodriguez E, Martinerie J, Varela FJ. 1999. Measuring phase synchrony in brain signals. Hum Brain Mapp. 8(4):194–208.

Lezak M. 2004. Neuropsychological Assessment. US: Oxford University Press.

Lobier M, Palva JM, Palva S. 2018. High-alpha band synchronization across frontal, parietal and visual cortex mediates behavioral and neuronal effects of visuospatial attention. Neuroimage. 165:222–237.

Mathewson KE, Beck DM, Fabiani M, Ro T, Gratton G. 2011. Pulsed out of awareness: EEG alpha oscillations represent a pulsed-inhibition of ongoing cortical processing. Front Psychol. 2:99.

Mazaheri A, Jensen O. 2010. Rhythmic pulsing: linking ongoing brain activity with evoked responses. Front Hum Neurosci. 4:177.

Miller EK, Cohen JD. 2001. An integrative theory of prefrontal cortex function. Annu Rev Neurosci. 24(1):167–202.

Mima T, Oluwatimilehin T, Hiraoka T, Hallett M. 2001. Transient interhemispheric neuronal synchrony correlates with object recognition. J Neurosci. 21(11):3942–3948.

Miyake A, Friedman NP, Emerson MJ, Witzki AH, Howerter A, Wager TD. 2000. The unity and diversity of executive functions and their contributions to complex 'Frontal Lobe' tasks: a latent variable analysis. Cognit Psychol. 41(1): 49–100.

Moll J, de Oliveira-Souza R, Moll FT, Bramati IE, Andreiuolo PA. 2002. The cerebral correlates of set-shifting: an FMRI study of the trail making test. Arq Neuropsiquiatr. 60(4):900–905.

Nolte G, Bai O, Wheaton L, Mari Z, Vorbach S, Hallett M. 2004. Identifying true brain interaction from EEG data using the imaginary part of coherency. Clin Neurophysiol. 115(10): 2292–2307.

Nomura EM, Gratton C, Visser RM, Kayser A, Perez F, D'Esposito M. 2010. Double dissociation of two cognitive control networks in patients with focal brain lesions. Proc Natl Acad Sci U S A. 107(26):12017–12022.

Oostenveld R, Fries P, Maris E, Schoffelen JM. 2010. FieldTrip: open source software for advanced analysis of MEG, EEG, and invasive electrophysiological data. Comput Intell Neurosci. 2011:156869.

Palva JM, Monto S, Kulashekhar S, Palva S. 2010. Neuronal synchrony reveals working memory networks and predicts individual memory capacity. Proc Natl Acad Sci USA. 107 (16):7580–7585.

Palva S, Palva JM. 2011. Functional roles of alpha-band phase synchronization in local and large-scale cortical networks. Front Psychol. 2:204.

Pang EW, Dunkley BT, Doesburg SM, da Costa L, Taylor MJ. 2016. Reduced brain connectivity and mental flexibility in mild traumatic brain injury. Ann Clin Transl Neurol. 3(2): 124–131.

Preti MG, Bolton TA, Van De Ville D. 2017. The dynamic functional connectome: state-of-the-art and perspectives. Neuroimage. 160:41–54.

Rorden C, Brett M. 2000. Stereotaxic display of brain lesions. Behav Neurol. 12(4):191–200.

Rorden C, Karnath HO. 2004. Using human brain lesions to infer function: a relic from a past era in the FMRI Age? Nat Rev Neurosci. 5(10):812–819.

Sadaghiani S, D'Esposito M. 2015. Functional characterization of the cingulo-opercular network in the maintenance of tonic alertness. Cereb Cortex. 25(9):2763–2773.

Sadaghiani S, Kleinschmidt A. 2016. Brain networks and α-oscillations: structural and functional foundations of cognitive control. Trends Cogn Sci. 20(11):805–817.

Sadaghiani S, Scheeringa R, Lehongre K, Morillon B, Giraud AL, D'Esposito M, Kleinschmidt A. 2012. Alpha-band phase synchrony is related to activity in the fronto-parietal adaptive control network. J Neurosci. 32(41):14305–14310.

Sadaghiani S, Scheeringa R, Lehongre K, Morillon B, Giraud AL, Kleinschmidt A. 2010. Intrinsic connectivity networks, alpha oscillations, and tonic alertness: a simultaneous electroencephalography/functional magnetic resonance imaging study. J Neurosci. 30(30):10243–10250.

Sauseng P, Klimesch W, Doppelmayr M, Pecherstorfer T, Freunberger R, Hanslmayr S. 2005. EEG alpha synchronization and functional coupling during top-down processing in a working memory task. Hum Brain Mapp. 26(2):148–155.

Scott WA. 1962. Cognitive complexity and cognitive flexibility. Sociometry. 25(4):405–414.

Seeley WW, Menon V, Schatzberg AF, Keller J, Glover GH, Kenna H, Reiss AL, Greicius MD. 2007. Dissociable intrinsic connectivity networks for salience processing and executive control. J Neurosci. 27(9):2349–2356.

Singer W. 2013. Cortical dynamics revisited. Trends Cogn Sci. 17(12):616–626.

Smit DJA, Linkenkaer-Hansen K, de Geus EJC. 2013. Long-range temporal correlations in resting-state alpha oscillations predict human timing-error dynamics. J Neurosci. 33(27): 11212–11220.

Sponheim SR, Clementz BA, Iacono WG, Beiser M. 2000. Clinical and biological concomitants of resting state EEG power abnormalities in schizophrenia. Biol Psychiatry. 48(11):1088–1097.

Stuss DT, Bisschop SM, Alexander MP, Levine B, Katz D, Izukawa D. 2001. The trail making test: a study in focal lesion patients. Psychol Assess. 13(2):230–239.

Uhlhaas PJ, Pipa G, Lima B, Melloni L, Neuenschwander S, Nikolić D, Singer W. 2009. Neural synchrony in cortical networks: history, concept and current status. Front Integr Neurosci. 3:17.

Varela F, Lachaux JP, Rodriguez E, Martinerie J. 2001. The Brainweb: phase synchronization and large-scale integration. Nat Rev Neurosci. 2(4):229–239.

Varjacic A, Mantini D, Demeyere N, Gillebert CR. 2018. Neural signatures of trail making test performance: evidence from lesion-mapping and neuroimaging studies. Neuropsychologia. 115:78–87.

von Stein A, Sarnthein J. 2000. Different frequencies for different scales of cortical integration: from local gamma to long range alpha/theta synchronization. Int J Psychophysiol. 38(3):301–313.

Wang XJ. 2010. Neurophysiological and computational principles of cortical rhythms in cognition. Physiol Rev. 90(3): 1195–1268.

Woltering S, Jung J, Liu Z, Tannock R. 2012. Resting state EEG oscillatory power differences in ADHD college students and their peers. Behav Brain Funct. 8(1):60.

Yochim B, Baldo J, Nelson A, Delis DC. 2007. D-KEFS trail making test performance in patients with lateral prefrontal cortex lesions. J Int Neuropsychol Soc. 13(4):704–709.

Zakzanis KK, Mraz R, Graham SJ. 2005. An FMRI study of the trail making test. Neuropsychologia. 43(13):1878–1886.

Zanto TP, Rubens MT, Thangavel A, Gazzaley A. 2011. Causal role of the prefrontal cortex in top-down modulation of visual processing and working memory. Nat Neurosci. 14: 656–661.